HHS Public Access

Author manuscript

Sci Transl Med. Author manuscript; available in PMC 2016 January 08.

Published in final edited form as:

Sci Transl Med. 2015 July 8; 7(295): 295ra109. doi:10.1126/scitranslmed.aab3881.

The proinflammatory role of HECTD2 in innate immunity and experimental lung injury

Tiffany A. Coon[1], **Alison C. McKelvey**[1], **Travis Lear**[1], **Shristi Rajbhandari**[1], **Sarah R. Dunn**[1], **William Connelly**[1], **Joe Y. Zhao**[1], **SeungHye Han**[1], **Yuan Liu**[1], **Nathaniel M. Weathington**[1], **Bryan J. McVerry**[1], **Yingze Zhang**[1], and **Bill B. Chen**[1,2,*]

[1]Department of Medicine, Acute Lung Injury Center of Excellence, University of Pittsburgh, Pittsburgh, PA 15213, USA.

[2]Vascular Medicine Institute, University of Pittsburgh, Pittsburgh, PA 15213, USA.

Abstract

Invading pathogens may trigger overactivation of the innate immune system, which results in the release of large amounts of proinflammatory cytokines (cytokine storm) and leads to the development of pulmonary edema, multiorgan failure, and shock. PIAS1 is a multifunctional and potent anti-inflammatory protein that negatively regulates several key inflammatory pathways such as Janus kinase (JAK)–signal transducer and activator of transcription (STAT) and nuclear factor κB (NF-κB). We discovered a ubiquitin E3 ligase, HECTD2, which ubiquitinated and mediated the degradation of PIAS1, thus increasing inflammation in an experimental pneumonia model. We found that GSK3b phosphorylation of PIAS1 provided a phosphodegron for HECTD2

*Corresponding author. chenb@upmc.edu.

SUPPLEMENTARY MATERIALS

www.sciencetranslationalmedicine.org/cgi/content/full/7/295/295ra109/DC1

Fig. S1. PIAS1 degradation occurs in a ubiquitin-dependent manner and through the proteasome.
Fig. S2. K30 is the ubiquitin acceptor site within PIAS1.
Fig. S3. Deletional mapping study identifying PIAS1 binding site within HECTD2.
Fig. S4. R397 is the preferred binding site for PIAS1.
Fig. S5. HECTD2 interacts with the first 20 amino acids of PIAS1.
Fig. S6. $HECTD2^{A19P}$ and deletional mutant localization study.
Fig. S7. FRET study of HECTD2 chimera proteins with PIAS1.
Fig. S8. BC1382 exhibits anti-inflammatory activity through preservation of PIAS1.
Fig. S9. BC1382 ameliorates LPS-induced lung injury.
Fig. S10. Source data for Fig. 1 (A to D and H).
Fig. S11. Source data for Fig. 2 (A to K).
Fig. S12. Source data for Fig. 3 (A to F).
Fig. S13. Source data for Figs. 4H, 5C, 6I, and 7 (C and I).
Table S1. Source sequencing data for Table 3.
Table S2. Source data for Fig. 1 (E to G).
Table S3. Source data for Fig. 3G.
Table S4. Source data for Fig. 4 (A to F).
Table S5. Source data for Fig. 5 (A, B, and D to F).
Table S6. Source data for Fig. 6 (A to G).
Table S7. Source data for Fig. 7 (C to G).

Author contributions: B.B.C. designed the study, analyzed the data, and wrote the manuscript. T.A.C., A.C.M., T.L., S.R., S.R.D., W.C., and J.Y.Z. performed all in vitro experiments and assisted with animal experiments. T.L. and Y.L. performed genetic analysis on ARDS cohorts. N.M.W., S.H., B.J.M., and Y.Z. assisted with human studies and S.H. performed statistical analysis. B.B.C. directed the study.

Competing interests: The authors declare that they have no competing financial interests.

targeting. We also identified a mislocalized HECTD2 polymorphism, *HECTD2*^{A19P}, that was present in 8.5% of the population and functioned to reduce inflammation. This polymorphism prevented HECTD2/PIAS1 nuclear interaction, thus preventing PIAS1 degradation. The HECTD2^{A19P} polymorphism was also protective toward acute respiratory distress syndrome (ARDS). We then developed a small-molecule inhibitor, BC-1382, that targeted HECTD2 and attenuated lipopolysaccharide (LPS)– and *Pseudomonas aeruginosa*–induced lung inflammation. These studies describe an unreported innate immune pathway and suggest that mutation or antagonism of the E3 ligase HECTD2 results in reduced severity of lung inflammation by selectively modulating the abundance of the anti-inflammatory protein PIAS1.

INTRODUCTION

PIAS [protein inhibitor of activated signal transducers and activators of transcription (STATs)] proteins are a family of multifunctional proteins that are known to negatively regulate several key inflammatory pathways in cells (1). Human PIAS proteins are encoded by four genes—*PIAS1*, *PIASx* (*PIAS2*), *PIAS3*, and *PIASy* (*PIAS4*) (1)—that are highly conserved. PIAS1 is known to suppress the activation of STATs and also binds to the p65 subunit of nuclear factor κB (NF-κB), preventing NF-κB–dependent gene activation (2–6). In addition, PIAS1 has small ubiquitin-like modifier E3 ligase activity in its RING-type domain, allowing it to function similarly to a ubiquitin E3 ligase by posttranslationally modifying specific substrates. PIAS1 knockout mice exhibit a significant increase in serum proinflammatory cytokines, even in unchallenged conditions (6), and adenovirus gene transfer of *PIAS1* was able to ameliorate severe acute pancreatitis (SAP)–associated acute lung injury (ALI) in rats, linking PIAS1 with pneumonia and lung inflammation (7). Overall, PIAS1 down-regulates inflammatory pathways at a variety of levels.

Ubiquitination of proteins is a posttranslational modification that influences a variety of housekeeping functions within the cell, the most common of which is the branding of proteins for proteasomal or lysosomal degradation (8). The mechanism of protein ubiquitination is dependent on 1 of more than 1000 E3 ligases divided into three domain subfamilies: RING finger, U-box, and HECT (9, 10). The existing ~30 HECT domain E3 ligases remain poorly characterized (11), and functional data are only available for a select few including E6AP, Smurf, and NEDD4 (11). Among these HECT E3 ligases, HECTD2 has been linked to prion disease, Alzheimer's disease, and prostate cancer (12–14). However, substrates of HECTD2 have not yet been identified. Here, we discovered a new pathway of innate immunity that presents HECTD2 as a crucial regulator of cytokine secretion by controlling the stability of anti-inflammatory PIAS1.

RESULTS

HECTD2 targets PIAS1 for ubiquitination, thereby increasing NF-κB signaling

PIAS1 degradation occurs in a ubiquitin-dependent manner and through the proteasome (fig. S1, A and B, and Fig. 1A). Through screening, we further determined that HECT domain E3 ligase HECTD2 expression decreased PIAS1 (fig. S1C). HECTD2 expression specifically decreased PIAS1 but not other isoforms (Fig. 1B); two randomly selected HECT E3 ligases,

KIAA0317 and HACE1, were also tested as negative controls (fig. S1D). Further, HECTD2 expression markedly decreased PIAS1's $t_{1/2}$, whereas HECTD2 knockdown using short hairpin RNA (shRNA) stabilized PIAS1 protein (Fig. 1C). The addition of purified HECTD2 with the full complement of E1 and E2 enzymes plus ubiquitin was sufficient to generate polyubiquitinated PIAS1 in vitro (Fig. 1D). Because the Cys residue within the *HECT domain* active site is required for transferring ubiquitin to the substrate (15, 16), we showed that HECTD2 C744S expression failed to decrease PIAS1 protein level (fig. S1E). Compared to wild-type (WT) and C749S mutant, HECTD2 C744S expression also did not decrease PIAS1's $t_{1/2}$ (fig. S1F). These studies suggest that C744S is a loss-of-function mutant, and C744 is a potential active site within HECTD2.

HECTD2 was detected in association with PIAS1 by coimmunoprecipitation (fig. S1G). Because PIAS1 is an important anti-inflammatory protein, we next investigated whether HECTD2 promotes inflammation. Indeed, HECTD2 overexpression drastically increased NF-κB promoter activity upon vehicle, lipopolysaccharide (LPS), tumor necrosis factor (TNF), or interferon-γ (IFN-γ) stimulation (Fig. 1E), whereas HECTD2 knockdown drastically reduced NF-κB promoter activity (Fig. 1F). Further, we transfected cells with PIAS1 shRNA 24 hours before HECTD2 overexpression. As shown in Fig. 1G, PIAS1 knockdown increased NF-κB promoter activity upon vehicle, LPS, TNF, or IFN-γ stimulation but completely abrogated any additional effects induced by HECTD2 overexpression. LPS treatment increased HECTD2 protein and decreased PIAS1 protein in murine lung epithelial (MLE) (Fig. 1H) and U937 cells (fig. S1H). LPS treatment also increased PIAS1's association to HECTD2 (Fig. 1H). Last, LPS treatment drastically increased *HECTD2* mRNA levels without changing the level of *PIAS1* mRNA (fig. S1I). LPS treatment also drastically decreased PIAS1 protein $t_{1/2}$ (fig. S1J). We further identified K30 as the ubiquitin acceptor site within PIAS1 (fig. S2A), because PIAS1 K30R exhibited resistance to ubiquitin and HECTD2 overexpression and an extended $t_{1/2}$ (fig. S2, B to D). PIAS1 K30R offered drastic resistance to HECTD2 and was able to suppress LPS-, TNF-, and IFN-induced NF-κB activation even upon coexpression with HECTD2 (fig. S2E).

We determined the PIAS1 binding site within the *N terminus* of HECTD2 (amino acids 393 to 397) (fig. S3, A to E). An alanine scan study within this region suggested that R397 is the preferred binding site for PIAS1, because $HECTD2^{R397A}$ drastically lost binding with PIAS1 (fig. S4A). Compared to $HECTD2^{WT}$, $HECTD2^{R397A}$ overexpression lost the ability to decrease PIAS1 protein levels (fig. S4B). $HECTD2^{R397A}$ overexpression also failed to accelerate PIAS1's $t_{1/2}$ (fig. S4C). These studies suggested that HECTD2 is an authentic E3 ligase that ubiquitinates PIAS1 and functions as a proinflammatory protein in vitro.

PIAS1 phosphorylation is required for HECTD2 targeting

We next investigated where HECTD2 targets PIAS1. We performed a similar mapping to fig. S3 using HECTD2 antibody to construct HECTD2 beads as the bait. We determined that HECTD2 interacts with the first 20 amino acids of PIAS1 (fig. S5, A to D). Database analysis indicated a candidate glycogen synthase kinase 3β (GSK3β) phosphorylation site within the *PIAS1 N-terminal SAP domain* (fig. S5E) [NetPhos 2.0 software prediction (17)]. GSK3β was detected in the PIAS1 immunoprecipitates (Fig. 2A). PIAS1 is also

phosphorylated at serine residue in cells (Fig. 2A). LPS drastically increased PIAS1 phosphorylation and GSK3β binding (Fig. 2, B and C). GSK3β knockdown using shRNA drastically stabilized PIAS1 protein in a cycloheximide $t_{1/2}$ study (Fig. 2D). WT GSK3β overexpression decreased PIAS1 protein levels in a dose-dependent manner; however, PIAS1 protein levels decreased more markedly when we transfected cells with a constitutively activated GSK3β hypermutant plasmid (Fig. 2E). Moreover, a cycloheximide $t_{1/2}$ study suggested that WT GSK3β ectopic expression decreased PIAS1's $t_{1/2}$ to ~2.5 hours, whereas the more potent GSK3β hypermutant further decreased PIAS1's $t_{1/2}$ to ~1 hour (Fig. 2F). Further, GSK3β knockdown protected PIAS1 from phosphorylation and degradation in LPS treatment (Fig. 2G). These studies suggested that GSK3β is an authentic regulator of PIAS1 protein stability. We further observed that GSK3β directly phosphorylated WT PIAS1, but not S13A, S17A, or S13/S17A mutant PIAS1, in an in vitro kinase assay (Fig. 2H). Compared to WT PIAS1, S13A and S17A mutants drastically decreased binding to HECTD2 (fig. S5F). These PIAS1 mutants also exhibited much longer half-lives (Fig. 2I), resisted degradation with HECTD2 coexpression (fig. S5G), and exhibited a marked decrease in phosphorylation and offered substantial protection against phosphorylation with LPS treatment (Fig. 2J and fig. S5H). Last, we performed a peptide binding experiment (Fig. 2K). Peptide with no phosphorylation (P1) and peptide with S13/S17A mutation (P4) were unable to bind to HECTD2; peptide with S17 phosphorylation (P3) offered drastically more HECTD2 binding compared to the peptide with S13 phosphorylation (P2). However, peptide with S13 phosphorylation (P2) offered drastically more GSK3β binding compared to the peptide with S17 phosphorylation (P3). Thus, PIAS1 phosphorylated S17 is the preferred binding site for HECTD2, whereas phosphorylated S13 is the preferred binding site for GSK3β.

HECTD2 contains a naturally occurring polymorphism at A19, which mislocalizes to the cytosol

The single-nucleotide polymorphism (SNP) database analysis indicated a naturally occurring nonsynonymous G/C polymorphism (rs7081569) within HECTD2 (A19P) with an allele frequency of 8.5% throughout the population (Table 1). To assess the behavior of $HECTD2^{A19P}$, we measured the ubiquitinating activity of the E3 ligase. Compared to $HECTD2^{WT}$, $HECTD2^{A19P}$ displayed a similar ability to polyubiquitinate PIAS1 (Fig. 3A). Also, both $HECTD2^{WT}$ and $HECTD2^{A19P}$ bind to PIAS1 in vitro (Fig. 3B). However, compared to $HECTD2^{WT}$, $HECTD2^{A19P}$ overexpression lost the ability to decrease PIAS1 protein level (Fig. 3C). Conditional expression of $HECTD2^{WT}$ in MLE cells using a doxycycline-inducible plasmid resulted in PIAS1 protein degradation upon doxycycline treatment. However, $HECTD2^{A19P}$ completely failed to decrease PIAS1 protein levels (Fig. 3, D and E). $HECTD2^{A19P}$ overexpression was not able to accelerate PIAS1 protein decay compared to $HECTD2^{WT}$ (Fig. 3F). Further, $HECTD2^{WT}$ plasmid transfection exacerbated the NF-κB pathway upon LPS and TNF treatment. In contrast, expression of $HECTD2^{A19P}$ did not markedly alter NF-κB promoter activity compared to that of cells transfected with the empty plasmid (Fig. 3G); thus, a naturally occurring $HECTD2^{A19P}$ polymorphism might confer a reduced proinflammatory phenotype. We hypothesized that $HECTD2^{A19P}$ loses its activity in cells due to mislocalization. Yellow fluorescent protein (YFP)–$HECTD2^{WT}$ exhibited comparable nuclear/cytosol signal, whereas YFP-$HECTD2^{A19P}$ almost completely

localized in the cytosol (Fig. 3H, upper panel). By isolating nuclear and cytosol fractions, we observed that HECTD2^{WT} distribution was comparable in both nuclear and cytosol fractions, whereas HECTD2^{A19P} distribution was exclusively in the cytosol fraction (fig. S6A).

We further tested the HECTD2/PIAS1 interaction in the nucleus by fluorescence resonance energy transfer (FRET) analysis using a photobleaching method (*18*). The results indicated that upon bleaching, there was decreased acceptor fluorescence (YPF) coupled with increased donor emission fluorescence [cyan fluorescent protein (CFP)], which suggest a HECTD2^{WT} interaction with PIAS1 within the nucleus in cells (Fig. 3H, lower panel). Because YFP-HECTD2^{A19P} almost completely resides in the cytosol, we did not observe any increased donor emission upon photobleaching in the nucleus. This suggested that nuclear entry of HECTD2 is required for PIAS1 targeting. Further deletional analysis indicated that the *N terminus* of HECTD2 is required for its nuclear entry, suggesting a potential nuclear localization signal (NLS) sequence within the first 20 to 40 amino acids of HECTD2 (fig. S6B). We also performed a rescue experiment by creating two chimera proteins YFP-HECTD2 R1 and YFP-HECTD2 R2 (fig. S7A) in which the first 40 amino acids of HECTD2^{WT} or CTP/phosphocholine cytidylyltransferase [CCTα; a known nuclear protein with *N-terminal NLS* (19)] were inserted in frame before YFP-HECTD2^{A19P}. Indeed, both YFP-HECTD2 R1 and YFP-HECTD2 R2 exhibited a comparable nuclear/cytosol signal (fig. S7B) and interacted with CFP-PIAS1 by FRET analysis (fig. S7C). Thus, nuclear entry of HECTD2 is both required and sufficient for PIAS1 targeting. This study also suggested that HECTD2^{A19P} is a loss-of-function polymorphism resulting from failed nuclear localization.

HECTD2^{A19P} is a loss-of-function E3 ligase polymorphism in vivo

So far, our in vitro studies suggest that HECTD2^{A19P} is a loss-of-function polymorphism. To extend the above observations in vivo, mice were infected with an empty lentivirus or lentivirus encoding either *HECTD2* or *HECTD2^{A19P}*. Mice were then challenged with *Pseudomonas aeruginosa* (PA103). *P. aeruginosa*, a gram-negative bacterium, is a significant contributor to nosocomial pneumonia (20), sepsis-associated ALI, and acute respiratory distress syndrome (ARDS) (21). Consequently, clinically isolated PA103 has been widely used in the animal model of ARDS (22–25). Mice were euthanized before analysis of parameters of inflammatory injury. HECTD2^{WT} expression, but not HECTD2^{A19P}, significantly augmented PA103-induced lung injury. Specifically, *HECTD2^{WT}* gene transfer significantly increased lavage protein concentrations and cell counts, and produced histologic evidence of severe lung inflammation (Fig. 4, A, B, and G). In addition, *HECTD2^{WT}* gene transfer significantly increased lavage cytokine levels compared to mice receiving an empty vector or *HECTD2^{A19P}* with PA103 infection (Fig. 4, D to F). Also, lentiviral gene transfer of empty, *HECTD2^{WT}*, or *HECTD2^{A19P}* did not significantly alter bacterial load (Fig. 4C). Last, HECTD2^{WT} drastically reduced PIAS1 protein expression in the lung, whereas HECTD2^{A19P} did not significantly alter PIAS1 levels compared to the empty control (Fig. 4H). All of the biologic effects, except bacterial loads, were less pronounced after gene transfer of *HECTD2^{A19P}*. These in vivo studies further support HECTD2^{A19P} as a loss-of-function polymorphism.

HECTD2^{A19P} polymorphism is characterized in ARDS patient cohorts

Because the HECTD2^{A19P} polymorphism offers blunted cytokine response in our animal model (Fig. 4), it is reasonable to hypothesize that HECTD2^{A19P} is a protective protein variant in patients who harbor the polymorphism. Strikingly, we sequenced the genomic DNA from 63 patients (47% male and 95% Caucasian) with or at-risk for ARDS and found 0 carriers for the *rs7081569* polymorphism (0 of 63). Examination of the HECTD2 genotype in the 1000 Genomes Project cohort (REF) demonstrated an 8.5% prevalence of the *rs7081569* polymorphism distributed evenly by gender ($P = 0.267$) but differentially by race ($P = 0.012$, Table 2). We performed the χ^2 test to examine the association between the *rs7081569* polymorphism in our ARDS cohort and control European descendants (Table 3 and table S1). The percentage of the genotypes *CG* or *CC* were significantly higher in the healthy controls (1000 Genomes Projects) compared to that in the ARDS cohort (13% versus 0%, $P = 0.003$), suggesting a potentially protective effect of the *C* allele in the *HECTD2* gene against the development of lung injury.

PIAS1 knockdown induces lung injury in vivo

To further confirm whether HECTD2 induces an inflammatory response through PIAS1 in vivo, mice were first infected with lentivirus encoding control shRNA or *PIAS1* shRNA and then challenged with LPS (intratracheally, 3 mg/kg). Both LPS and PIAS1 knockdown significantly increased lavage protein concentrations, lavage cell counts, lavage cytokines, and cell infiltrates (Fig. 5, A, B, and D to G). Further, PIAS1 knockdown significantly exacerbated lavage cell counts, TNF levels, and cell infiltrates induced by LPS (Fig. 5, B, D, and G) without affecting lavage protein, IL-1, or IL-6 levels compared to the control shRNA (Fig. 5, A, E, and F). We also showed that innate murine lungs have very low levels of HECTD2, which increase significantly upon LPS stimulation (Fig. 5C). Both LPS and lentivirus encoding *PIAS1* shRNA effectively reduce PIAS1 protein levels (Fig. 5C). Collectively, this experiment suggested that PIAS1 is an important suppressor of inflammation in the lung, and HECTD2 induces an inflammatory response in the lung partially through PIAS1.

HECTD2 knockdown ameliorates *Pseudomonas*-induced lung injury in vivo

To further confirm the role of HECTD2 in pneumonia and evaluate whetherHECTD2 is required in lung inflammation, we pursued in vivo knockdown studies. Mice were first infected with lentivirus encoding control shRNA or *HECTD2* shRNA and then challenged with PA103. HECTD2 knockdown significantly decreased lavage protein concentrations, lavage cell counts, and cell infiltrates without affecting bacterial load (Fig. 6, A to C and H). Further, HECTD2 knockdown significantly decreased lavage cytokine levels in PA103-infected mice (Fig. 6, D to F), and these mice had improved survival (Fig. 6G). Last, lentivirus encoding *HECTD2* shRNA effectively reduced HECTD2 protein level against PA103 infection, leading to an increase in PIAS1 protein level in the lung (Fig. 6I). Collectively, the above studies suggest for the first time that HECTD2 plays an integral role in mediating cytokine-driven inflammation via the PIAS1-cytokine axis and may serve as a potential pharmaceutical target.

A small-molecule inhibitor of HECTD2 exhibits anti-inflammatory activity

HECTD2 harbors a conserved *HECT domain* within its *C terminus* (11, 26). Because the *HECT domain* carries out the E3 ligase activity of transferring ubiquitin to the substrate (11, 26), we hypothesized that small-molecule inhibition of the *HECT domain* would disrupt HECTD2 targeting its substrate, PIAS1. We first constructed a homology model using the *NEDD4 HECT domain* (27, 28) (2XBF.pdb) (Fig. 7A). Using molecular docking analysis and score-ranking operations on the predicted *HECTD2-HECT domain* three-dimensional structure model, we assessed potential ligands that might fit the *HECT domain* cavities (Fig. 7B). Through the LibDock program from Discovery Studio 3.5, we were able to screen the potential ligands for the *HECTD2-HECT domain*. G723, K470, and T526 residues within the *HECT domain* are important for interacting with inhibitors (fig. S8A). We were able to test one of the selected compounds, termed BC-1382, in an in vitro binding assay (Fig. 7C). The result suggested that BC-1382 is a potent inhibitor of HECTD2 with IC_{50} (median inhibitory concentration) ≈ 5 nM toward disrupting the HECTD2/PIAS1 interaction. BC-1382 drastically increased PIAS1 protein level in a nonstimulus condition with IC_{50} ≈100 nM (fig. S8B). PIAS3, PIAS4, and HECTD2 protein levels appeared to be unchanged. BC-1382 did not alter mRNA levels of *PIAS1*, *PIAS4*, or *HECTD2* (fig. S8C). BC-1382 also improved PIAS1 protein stability by increasing its $t_{1/2}$ (fig. S8D). BC-1382 suppressed LPS-induced PIAS1 degradation and restored PIAS1 protein levels at 800 nM (fig. S8E). Last, BC-1382 was able to suppress LPS-induced proinflammatory cytokines released by human peripheral blood mononuclear cells (PBMCs) (fig. S8F). To assess the in vivo anti-inflammatory activity of BC-1382, we tested it using *P. aeruginosa*– and LPS-induced pneumonia models. Briefly, C57BL/6J mice were challenged intratracheally with PA103 (10^4 CFU per mouse) or LPS (3 mg/kg). BC-1382 was given through intraperitoneal injection (10 mg/kg) at the same time. Eighteen hours later, mice were euthanized, and lungs were lavaged with saline. BC-1382 did not appear to affect BAL bacteria (Fig. 7D). However, it significantly decreased lavage protein concentrations, lavage cell counts, and cell infiltrates in both PA103-stimulated (Fig. 7, E, F, and H) and LPS-stimulated (fig. S9, A, B, and D) mice. Further, BC-1382 significantly decreased lavage cytokine levels in both models (Fig. 7G and fig. S9C). Last, PA103 very effectively increased HECTD2 protein level and decreased PIAS1 in the lung. However, PIAS1 protein level is preserved by BC-1382 (Fig. 7I). Hence, small-molecule targeting of the HECTD2-PIAS1 pathway reduces the severity of cytokine-driven lung inflammation (Fig. 8).

DISCUSSION

An overactivated innate immune system triggered by invading pathogens will release large amounts of proinflammatory cytokines (that is, cytokine storm), leading to the devastating effects of pulmonary edema, multiorgan failure, and shock (29, 30). Current efforts using systemic corticosteroids to block cytokine storm have shown many side effects in clinical trials (31). Other biological approaches (for example, TNF-α and TNF receptor antibodies) are greatly limited because only one target (a receptor or cytokine) is selected for inhibition (*32*). However, many inflammatory diseases are intricate disorders, whereby a combination of inflammatory mediators is released from the activation of multiple receptors. Hence, there is an unmet scientific need to discover a molecular target that could lead to a new generation

of agents that can potently modulate innate immunity and the host inflammatory response. This study provides a link between HECTD2 and PIAS1 in innate immunity and sets the stage for future analysis of HECTD2 polymorphisms in a much bigger cohort of patients with many other inflammatory diseases.

We showed that HECTD2 is a bona fide E3 ligase that triggers the ubiquitination and degradation of PIAS1 for exacerbated inflammation in vivo and in vitro. In essence, HECTD2 appeared to promote inflammation in part by destabilizing PIAS1, thus preventing it from controlling transcriptional regulatory pathways like NF-κB. PIAS1 knockdown itself is sufficient to increase NF-κB promoter activity upon vehicle, LPS, TNF, or IFN-γ stimulation, but it totally abrogated any additional effects induced by HECTD2 overexpression (Fig. 1G). An in vivo study also suggested that PIAS1 is an important suppressor of inflammation in the lung, and HECTD2 induces an inflammatory response in the lung partially through PIAS1. Moreover, GSK3β was found as a regulator that phosphorylates PIAS1, thereby serving as a molecular signal for HECTD2 targeting. Specifically, phosphorylated S13 is the preferred binding site for GSK3β, whereas phosphorylated S17 is the preferred binding site for HECTD2 (Fig. 2K). It is highly likely that PIAS1 S13 is a priming phosphorylation site by another kinase(s) for GSK3β binding, which leads to the phosphorylation of S17. The latter motif served as the phosphodegron for HECTD2 targeting. Similar mechanisms of substrate targeting by GSK3β phosphodegron motifs have been described (33, 34). Previous studies of PIAS1 activity upon proinflammatory stimuli identified the IκB kinase α (IKKα)–mediated phosphorylation of PIAS1 at S90 to swiftly repress inflammatory gene transcription (3). However, this phosphorylation occurred very rapidly (within 10 to 30 min) (*3*). Our study, however, found that GSK3β regulates PIAS1 protein stability and describes a mechanism of PIAS1 basal protein turnover controlled constitutively by HECTD2, providing an internal checkpoint for the cell to shut off the anti-inflammatory pathway, a mechanism hijacked by endotoxins to shut down PIAS1 and propel cytokine storm.

We revealed a naturally occurring amino acid variant in HECTD2 that is present at a frequency of ~8.5% of the population (HECTD2^{A19P}). This loss-of-function polymorphism causes the mislocalization of itself in the cytosol, leaving it unable to enter the nucleus where PIAS1 continues its anti-inflammatory activity. So far, many genetic diseases have been linked to the mislocalization of nuclear proteins because of SNPs within the NLS region (35). For example, missense mutations within the NLS of sex-determining region Y protein (SRY) that reduce the nuclear localization of SRY have been characterized in patients with Swyer syndrome (36). However, our preliminary results based on our ARDS cohorts (63 patients) showed that the HECTD2^{A19P} polymorphism is a protected mutant, at least in the disease of ARDS. One of the clinical hallmarks of patients with pneumonia- or sepsis-induced ARDS is a robust acute host inflammatory response triggered by invading pathogens (37). Specifically, the innate immune system is triggered to secrete large amounts of proinflammatory cytokines (that is, cytokine storm), which further causes tissue injury and organ failure (38). The HECTD2^{A19P} polymorphism offers blunted cytokine response in our animal model (Fig. 4), which is consistent with the fact that HECTD2^{A19P} is a protective protein variant in ARDS patients who harbor the polymorphism. Further prospective study

in disease cohorts is required to validate this observation. HECTD2^{A19P} may also be an important and protective polymorphism in many other inflammatory diseases.

The discovery of HECTD2 as a stimulator of proinflammatory signaling provided the mechanistic platform that led to the design, synthesis, and biological evaluation of a first-in-class small-molecule inhibitor that exerted robust anti-inflammatory activity by impairing cytokine release. We developed a small-molecule inhibitor of HECTD2, BC-1382, by using the readily available NEDD4 HECT crystal structure to generate a homology model of *HECTD2 C-terminal structure*. We had previously used a similar approach to design inhibitors for the proinflammatory protein FBXO3 (29, 30). BC-1382 was able to drastically attenuate LPS- and *P. aeruginosa*–induced lung injury (Fig. 7 and fig. S9). Future studies will focus on evaluating the safety profile, distribution, elimination, and metabolism of this chemical entity in other inflammatory models beyond pneumonia and sepsis. Successful results from these studies will provide the basis for translating to clinical application in acute and chronic inflammatory illness.

MATERIALS AND METHODS

Study design

Our goal in this study was to investigate the role of HECTD2 in innate immunity and models of experimental lung injury. Several in vitro approaches were used to determine the proinflammatory function of HECTD2. We also determined the molecular interplay between HECTD2 and its substrate, PIAS1. To further test HECTD2 in vivo, C57BL6 mice were given lentivirus encoding *HECTD2*, *A19P variant*, or *HECTD2* shRNA. Seven days later, mice were infected with *P. aeruginosa* to mimic the lung injury. Mice were randomized in different groups, but the experimenter was not blinded to the group identities. Human genomic DNA was also collected and isolated from subjects diagnosed with ARDS after obtaining informed consent. We tried to differentiate the HECTD2 *A19P* polymorphism in healthy and ARDS patient cohorts.

Materials

Sources of the MLE, A549, and 293T cell lines were described previously (39, 40). Purified ubiquitin, E1, E2, MG132, leupeptin, and cycloheximide were purchased from Calbiochem. Mouse monoclonal V5 antibody, the pcDNA3.1D cloning kit, *E. coli* One Shot competent cells, the pENTR Directional TOPO cloning kits, Gateway mammalian expression system, and genomic extraction kit were from Invitrogen. Fluorescent vector pAmCyan1-C1 and pZsYellow1-N1 and Lentivirus kit were from Clontech. PBMCs were from Sanguine Life Sciences. The *HECT domain* E3 ligase complementary DNA, scramble shRNA, *HECTD2*, *PIAS1*, and *GSK3*β shRNA sets were purchased from Open Biosystems. Nucleofector transfection kits were from Amaxa. Immobilized protein A/G beads were from Pierce. In vitro transcription and translation (TnT) kits were from Promega. The Cignal NF-κB Reporter Luciferase Kit (CCS-013L) was from Qiagen. Complete proteasome inhibitors were from Roche. HECTD2 antibodies were from Abcam and Santa Cruz Biotechnology. PIAS and GSK3β antibodies were from Cell Signaling and Santa Cruz Biotechnology. IL-1β, TNF-α, and IL-6 mouse ELISA kit, human cytokine array, and TNF-α and IFN-γ

proteins were from R&D Systems. LPS (*E. coli*) was from Sigma. Peptides were custom-synthesized from CHI Scientific. DNA sequencing was performed at Genewiz. All small-molecule compound analysis was performed by the University of Pittsburgh Mass Spectrometry and Nuclear Magnetic Resonance facility.

Human samples

This study was approved by the University of Pittsburgh Institutional Review Board. After obtaining informed consent, we collected blood from subjects diagnosed with ARDS (clinical diagnosis). Genomic DNA was isolated from whole blood (Puregene DNA Isolation Kit, Qiagen).

Cell culture

MLE cells were cultured in Dulbecco's modified Eagle's medium–F12 (Gibco) supplemented with 10% fetal bovine serum (DMEM-10). PBMCs were thawed and cultured in RPMI medium supplemented with 10% fetal bovine serum following the manufacturer's protocol (Sanguine Life Sciences). For HECTD2 overexpression in 293T cells, Fugene6HD transfection reagent was used following the manufacturer's protocol. Twenty-four hours later, cells were treated with LPS at 0 to10 μg/ml, TNF at 10 ng/ml, or IFN-γ at 10 ng/ml for an additional 18 hours. For HECTD2 or GSK3β knockdown studies in MLE cells, scramble, *HECTD2*, or *GSK3*β shRNA was used to transfect cells for 48 hours using electroporation. For drug treatment, compounds were solubilized in dimethyl sulfoxide before being added to the cells for up to 18 hours. Cell-free medium was collected and analyzed for cytokine release. Cell lysates were prepared by brief sonication in 150 mM NaCl, 50 mM tris, 1.0 mM EDTA, 2 mM dithiothreitol (DTT), 0.025% sodium azide, and 1 mM phenylmethylsulfonyl fluoride (buffer A) at 4°C. For half-life study, MLE cells were exposed to cycloheximide (40 μg/ml) in a time-dependent manner for up to 6 hours. Cells were then collected and assayed for HECTD2 or PIAS1 immunoblotting.

In vitro protein binding assays

PIAS1 protein was immunoprecipitated from 1 mg of cell lysate using PIAS1 antibody (rabbit) and coupled to protein A/G beads. PIAS1 beads were then incubated with in vitro synthesized products (50 μl) expressing HIS-V5-HECTD2 mutants. After washing, proteins were eluted and processed for V5-HECTD2 immunoblotting. Similarly, HECTD2 was immunoprecipitated from 1 mg of cell lysate using HECTD2 antibody (goat) and coupled to protein A/G beads. HECTD2 beads were then incubated with in vitro synthesized products (50 μl) expressing HIS-V5-PIAS1 mutants. After washing, proteins were eluted and processed for V5-PIAS1 immunoblotting.

In vitro peptide binding assays

Biotin-labeled peptides were first coupled to streptavidin-agarose beads for 1 hour. Beads were then incubated with purified HECTD2 or GSK3β for 18 hours. After washing, proteins were eluted and processed for V5-HECTD2 or GSK3β immunoblotting.

In vitro ubiquitin conjugation assays

The assay was performed in a volume of 25 μl containing 50 mM tris (pH 7.6), 5 mM $MgCl_2$, 0.6 mM DTT, 2 mM adenosine triphosphate, E1 (1.5 ng/μl), Ubc5 (10 ng/μl), Ubc7 (10 ng/μl), ubiquitin (1 μg/μl) (Calbiochem), 1 μM ubiquitin aldehyde, and in vitro synthesized V5-PIAS1 and HECTD2. Reaction products were processed for V5 immunoblotting.

NF-κB promoter assay

Cignal NF-κB Reporter luciferase plasmids were cotransfected with empty, *HECTD2*, control shRNA, *PIAS1* shRNA, or *HECTD2* shRNA for 24 to 48 hours before vehicle, LPS, TNF, or IFN-γ treatment for an additional 6 to 18 hours. Cells were then collected and assayed for firefly and *Renilla* luciferase activity. NF-κB promoter activity was normalized by firefly and *Renilla* luciferase activity ratio.

Molecular docking studies and compound design

The docking experiments were carried out by using software from Discovery Studio 3.5. A library containing 500,000 approved or experimental drugs was first used to screen potential ligands for HECTD2. *HECTD2-HECT domain* structural analysis revealed several potential binding cavities for inhibitor targeting. These binding cavities were adopted into the LibDock algorithm to screen for the optimum inhibitor. On the basis of the docking and best-fit analysis of suitable ligands, BC-1382 and other high-scoring molecules were selected and further tested in vitro.

Real-time quantitative polymerase chain reaction, cloning, and mutagenesis

Total RNA was isolated and reverse transcription was performed followed by real-time quantitative polymerase chain reaction (qPCR) with SYBR Green qPCR mixture as described (41). All mutant *PIAS1* and *HECTD2* plasmid constructs were generated using PCR-based approaches using appropriate primers and subcloned into a pcDNA3.1D/V5-His vector.

Lentivirus construction

To generate lentivirus encoding *HECTD2*, Plvx-HECTD2 plasmid was cotransfected with Lenti-X HTX packaging plasmids (Clontech) into 293FT cells following the manufacturer's instructions. Seventy-two hours later, virus was collected and concentrated using Lenti-X concentrator.

Cytokine arrays

Cytokine Array, Panel A (R&D Systems) was used to profile 36 cytokines in cell-free medium or murine lavage. Each cytokine signal value was quantified using ImageJ software on the basis of the relative signal intensities and graphed.

SNP genotyping

To elucidate the genotype of acute lung injury patients, we amplified a 700–base pair DNA fragment flanking the *rs7081569* polymorphism in the *HECTD2* gene using genomic DNA

(n = 63), and the forward primer ATGAGTGAGGCGGTTCGGGT and reverse primer TGTACCATATGAAAAATAAAACCATCACTGATG. These PCR products were analyzed using agarose gel electrophoresis, and the correct DNA fragment was collected and purified using the Qiagen Gene Clean Kit. The purified PCR product was sequenced with an internal primer TCCCAACTCCCGCCGT through the company Genewiz.

FRET analysis

Cells were plated and cotransfected with CFP-*PIAS1* and YFP- *HECTD2*^{Wt} or YFP-*HECTD2*^{A19P} plasmids as described (18, 40). Interactions were detected at the single-cell level by using a combination laser-scanning microscope system (Nikon A1). Briefly, MLE cells were transfected with CFP and YFP plasmid for 24 hours. Cells were fixed with 4% paraformaldehyde for 10 min. To achieve excitation, the 458- or 514-nm line of an argon ion laser was focused through the ×60 oil differential interference contrast objective lens onto the cell. Emissions of CFP (the FRET donor) and YFP (the FRET acceptor) were collected, respectively. Photobleaching was performed with 100% intensity of a 514-nm laser for 2 s. FRET quantitation of fluorescence images was generated using Nikon NIS-Elements software. Here, the emission fluorescence of both the donor CFP-PIAS1 and acceptor YFP-HECTD2 (Fig. 3H) before and after acceptor photobleaching was measured around the region of interest (nucleus, marked in red arrow). Positive FRET is indicated by the decreased acceptor fluorescence (YPF) coupled with increased donor emission fluorescence (CFP) upon photobleaching.

Animal studies

All procedures were approved by the University of Pittsburgh Institutional Animal Care and Use Committee. For pneumonia studies, C57BL6 mice were deeply anesthetized using a ketamine/xylazine mixture, and the larynx was well visualized under a fiber optic light source before endotracheal intubation with a 3/400 24-gauge plastic catheter. Lentivirus (10^7 CFU) encoding genes for *HECTD2*, *HECTD2*^{A19P}, or *HECTD2* shRNA was instilled intratracheally for 144 hours before administration of *P. aeruginosa* (strain PA103, 10^4 CFU per mouse, intratracheally) for 18 hours, after which animals were euthanized and assayed for BAL protein, cell count, bacterial count, cytokines, and lung infiltrates (29, 30, 34). Survival studies of mice were performed on mice that were given *P. aeruginosa* (strain PA103, 10^5 CFU per mouse, intratracheally, 8 mice per group). Mice were carefully monitored over time; moribund, preterminal animals were immediately euthanized and recorded as deceased. For drug studies, mice were deeply anesthetized as above. PA103 (10^4 CFU) or LPS (3 mg/kg) was instilled intratracheally before BC-1382 (10 mg/kg) was administered to the mice through an intraperitoneal injection. Eighteen hours later, animals were euthanized and analyzed as above.

Statistical analysis

Statistical comparisons were performed with mean ± SEM for continuous variables. All data were statistically analyzed by unpaired Student's t test. Kaplan-Meier survival curves were generated for animal studies. χ^2 test was used to analyze human data. All analyses will be performed using SPSS (IBM) or Stata Statistical Software: Release 10.1 (StataCorp LP).

Supplementary Material

Refer to Web version on PubMed Central for supplementary material.

Acknowledgments

Funding: This work was supported by the NIH R01 grant HL116472 (to B.B.C.), P01 grant HL114453 (to B.B.C., B.J.M., and Y.Z.), and the University of Pittsburgh Vascular Medicine Institute seed fund.

REFERENCES AND NOTES

1. Rytinki MM, Kaikkonen S, Pehkonen P, Jääskeläinen T, Palvimo JJ. PIAS proteins: Pleiotropic interactors associated with SUMO. Cell. Mol. Life Sci. 2009; 66:3029–3041. [PubMed: 19526197]
2. Liu B, Shuai K. Targeting the PIAS1 SUMO ligase pathway to control inflammation. Trends Pharmacol. Sci. 2008; 29:505–509. [PubMed: 18755518]
3. Liu B, Yang Y, Chernishof V, Loo RR, Jang H, Tahk S, Yang R, Mink S, Shultz D, Bellone CJ, Loo JA, Shuai K. Proinflammatory stimuli induce IKKα-mediated phosphorylation of PIAS1 to restrict inflammation and immunity. Cell. 2007; 129:903–914. [PubMed: 17540171]
4. Liu B, Liao J, Rao X, Kushner SA, Chung CD, Chang DD, Shuai K. Inhibition of Stat1-mediated gene activation by PIAS1. Proc. Natl. Acad. Sci. U.S.A. 1998; 95:10626–10631. [PubMed: 9724754]
5. Liu Y, Zhang YD, Guo L, Huang HY, Zhu H, Huang JX, Liu Y, Zhou SR, Dang YJ, Li X, Tang QQ. Protein inhibitor of activated STAT 1 (PIAS1) is identified as the SUMO E3 ligase of CCAAT/enhancer-binding protein β (C/EBPβ) during adipogenesis. Mol. Cell. Biol. 2013; 33:4606–4617. [PubMed: 24061474]
6. Liu B, Yang R, Wong KA, Getman C, Stein N, Teitell MA, Cheng G, Wu H, Shuai K. Negative regulation of NF-κB signaling by PIAS1. Mol. Cell. Biol. 2005; 25:1113–1123. [PubMed: 15657437]
7. Chen P, Huang L, Sun Y, Yuan Y. Upregulation of PIAS1 protects against sodium taurocholate-induced severe acute pancreatitis associated with acute lung injury. Cytokine. 2011; 54:305–314. [PubMed: 21419645]
8. Tanaka Y, Tanaka N, Saeki Y, Tanaka K, Murakami M, Hirano T, Ishii N, Sugamura K. c-Cbl-dependent monoubiquitination and lysosomal degradation of gp130. Mol. Cell. Biol. 2008; 28:4805–4818. [PubMed: 18519587]
9. Jin J, Li X, Gygi SP, Harper JW. Dual E1 activation systems for ubiquitin differentially regulate E2 enzyme charging. Nature. 2007; 447:1135–1138. [PubMed: 17597759]
10. Hatakeyama S, Yada M, Matsumoto M, Ishida N, Nakayama KI. U box proteins as a new family of ubiquitin-protein ligases. J Biol. Chem. 2001; 276:33111–33120. [PubMed: 11435423]
11. Rotin D, Kumar S. Physiological functions of the HECT family of ubiquitin ligases. Nat. Rev. Mol. Cell Biol. 2009; 10:398–409. [PubMed: 19436320]
12. Lloyd SE, Maytham EG, Pota H, Grizenkova J, Molou E, Uphill J, Hummerich H, Whitfield J, Alpers MP, Mead S, Collinge J. *HECTD2* is associated with susceptibility to mouse and human prion disease. PLOS Genet. 2009; 5:e1000383. [PubMed: 19214206]
13. Lloyd SE, Rossor M, Fox N, Mead S, Collinge J. HECTD2, a candidate susceptibility gene for Alzheimer's disease on 10q. BMC Med. Genet. 2009; 10:90. [PubMed: 19754925]
14. Sun T, Wang X, He HH, Sweeney CJ, Liu SX, Brown M, Balk S, Lee GS, Kantoff PW. MiR-221 promotes the development of androgen independence in prostate cancer cells via downregulation of HECTD2 and RAB1A. Oncogene. 2014; 33:2790–2800. [PubMed: 23770851]
15. Zheng N, Wang P, Jeffrey PD, Pavletich NP. Structure of a c-Cbl–UbcH7 complex: RING domain function in ubiquitin-protein ligases. Cell. 2000; 102:533–539. [PubMed: 10966114]
16. Li W, Tu D, Brunger AT, Ye Y. A ubiquitin ligase transfers preformed polyubiquitin chains from a conjugating enzyme to a substrate. Nature. 2007; 446:333–337. [PubMed: 17310145]

17. Blom N, Gammeltoft S, Brunak S. Sequence and structure-based prediction of eukaryotic protein phosphorylation sites. J Mol. Biol. 1999; 294:1351–1362. [PubMed: 10600390]
18. Coon TA, Glasser JR, Mallampalli RK, Chen BB. Novel E3 ligase component FBXL7 ubiquitinates and degrades Aurora A, causing mitotic arrest. Cell Cycle. 2012; 11:721–729. [PubMed: 22306998]
19. Chen BB, Mallampalli RK. Masking of a nuclear signal motif by monoubiquitination leads to mislocalization and degradation of the regulatory enzyme cytidylyltransferase. Mol. Cell. Biol. 2009; 29:3062–3075. [PubMed: 19332566]
20. Ibrahim EH, Ward S, Sherman G, Kollef MH. A comparative analysis of patients with early-onset vs late-onset nosocomial pneumonia in the ICU setting. Chest. 2000; 117:1434–1442. [PubMed: 10807834]
21. Meduri GU, Reddy RC, Stanley T, El-Zeky F. Pneumonia in acute respiratory distress syndrome. A prospective evaluation of bilateral bronchoscopic sampling. Am. J. Respir. Crit. Care Med. 1998; 158:870–875. [PubMed: 9731019]
22. Sawa T, Corry DB, Gropper MA, Ohara M, Kurahashi K, Wiener-Kronish JP. IL-10 improves lung injury and survival in *Pseudomonas aeruginosa* pneumonia. J Immunol. 1997; 159:2858–2866. [PubMed: 9300709]
23. Kurahashi K, Kajikawa O, Sawa T, Ohara M, Gropper MA, Frank DW, Martin TR, Wiener-Kronish JP. Pathogenesis of septic shock in *Pseudomonas aeruginosa* pneumonia. J Clin. Invest. 1999; 104:743–750. [PubMed: 10491409]
24. Pankhaniya RR, Tamura M, Allmond LR, Moriyama K, Ajayi T, Wiener-Kronish JP, Sawa T. *Pseudomonas aeruginosa* causes acute lung injury via the catalytic activity of the patatin-like phospholipase domain of ExoU. Crit. Care Med. 2004; 32:2293–2299. [PubMed: 15640644]
25. Chen BB, Coon TA, Glasser JR, Mallampalli RK. Calmodulin antagonizes a calcium-activated SCF ubiquitin E3 ligase subunit, FBXL2, to regulate surfactant homeostasis. Mol. Cell. Biol. 2011; 31:1905–1920. [PubMed: 21343341]
26. Huang L, Kinnucan E, Wang G, Beaudenon S, Howley PM, Huibregtse JM, Pavletich NP. Structure of an E6AP-UbcH7 complex: Insights into ubiquitination by the E2–E3 enzyme cascade. Science. 1999; 286:1321–1326. [PubMed: 10558980]
27. Umadevi N, Kumar S, Narayana N. Crystallization and preliminary X-ray diffraction studies of the WW4 domain of the Nedd4-2 ubiquitin-protein ligase. Acta Crystallogr. Sect. F Struct. Biol. Cryst. Commun. 2005; 61:1084–1086.
28. Kamadurai HB, Souphron J, Scott DC, Duda DM, Miller DJ, Stringer D, Piper RC, Schulman BA. Insights into ubiquitin transfer cascades from a structure of a UbcH5B ~ubiquitin-HECT^{NEDD4L} complex. Mol. Cell. 2009; 36:1095–1102. [PubMed: 20064473]
29. Mallampalli RK, Coon TA, Glasser JR, Wang C, Dunn SR, Weathington NM, Zhao J, Zou C, Zhao Y, Chen BB. Targeting F box protein Fbxo3 to control cytokine-driven inflammation. J Immunol. 2013; 191:5247–5255. [PubMed: 24123678]
30. Chen BB, Coon TA, Glasser JR, McVerry BJ, Zhao J, Zhao Y, Zou C, Ellis B, Sciurba FC, Zhang Y, Mallampalli RK. A combinatorial F box protein directed pathway controls TRAF adaptor stability to regulate inflammation. Nat. Immunol. 2013; 14:470–479. [PubMed: 23542741]
31. Annane D, Cavaillon JM. Corticosteroids in sepsis: From bench to bedside? Shock. 2003; 20:197–207. [PubMed: 12923489]
32. Eichacker PQ, Parent C, Kalil A, Esposito C, Cui X, Banks SM, Gerstenberger EP, Fitz Y, Danner RL, Natanson C. Risk and the efficacy of antiinflammatory agents: Retrospective and confirmatory studies of sepsis. Am. J. Respir. Crit. Care Med. 2002; 166:1197–1205. [PubMed: 12403688]
33. Frame S, Cohen P, Biondi RM. A common phosphate binding site explains the unique substrate specificity of GSK3 and its inactivation by phosphorylation. Mol. Cell. 2001; 7:1321–1327. [PubMed: 11430833]
34. Zhao J, Wei J, Mialki RK, Mallampalli DF, Chen BB, Coon T, Zou C, Mallampalli RK, Zhao Y. F-box protein FBXL19–mediated ubiquitination and degradation of the receptor for IL-33 limits pulmonary inflammation. Nat. Immunol. 2012; 13:651–658. [PubMed: 22660580]

35. Hung MC, Link W. Protein localization in disease and therapy. J Cell Sci. 2011; 124:3381–3392. [PubMed: 22010196]

36. Harley VR, Layfield S, Mitchell CL, Forwood JK, John AP, Briggs LJ, McDowall SG, Jans DA. Defective importin β recognition and nuclear import of the sex-determining factor SRY are associated with XY sex-reversing mutations. Proc. Natl. Acad. Sci. U.S.A. 2003; 100:7045–7050. [PubMed: 12764225]

37. Lorente JA, Marshall JC. Neutralization of tumor necrosis factor in preclinical models of sepsis. Shock. 2005; 24:107–119. [PubMed: 16374382]

38. Sheu CC, Gong MN, Zhai R, Bajwa EK, Chen F, Thompson BT, Christiani DC. The influence of infection sites on development and mortality of ARDS. Intensive Care Med. 2010; 36:963–970. [PubMed: 20229040]

39. Ray NB, Durairaj L, Chen BB, McVerry BJ, Ryan AJ, Donahoe M, Waltenbaugh AK, O'Donnell CP, Henderson FC, Etscheidt CA, McCoy DM, Agassandian M, Hayes-Rowan EC, Coon TA, Butler PL, Gakhar L, Mathur SN, Sieren JC, Tyurina YY, Kagan VE, McLennan G, Mallampalli RK. Dynamic regulation of cardiolipin by the lipid pump Atp8b1 determines the severity of lung injury in experimental pneumonia. Nat. Med. 2010; 16:1120–1127. [PubMed: 20852622]

40. Chen BB, Mallampalli RK. Calmodulin binds and stabilizes the regulatory enzyme, CTP: Phosphocholine cytidylyltransferase. J Biol. Chem. 2007; 282:33494–33506. [PubMed: 17804406]

41. Butler PL, Mallampalli RK. Cross-talk between remodeling and de novo pathways maintains phospholipid balance through ubiquitination. J Biol. Chem. 2010; 285:6246–6258. [PubMed: 20018880]

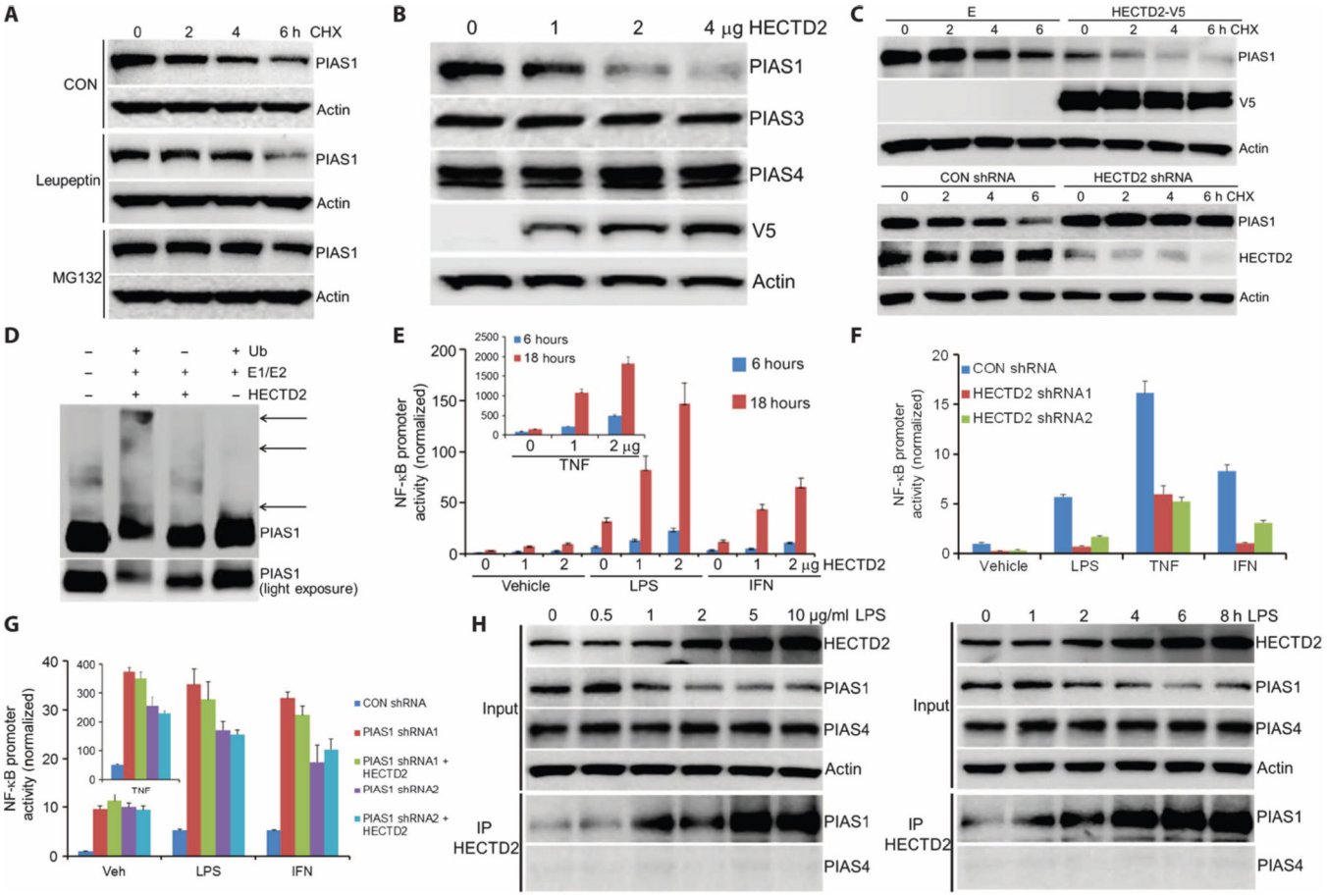

Fig. 1. HECTD2 targets PIAS1 for polyubiquitination, thereby increasing NF-κB signaling

(**A**) Endogenous PIAS1 protein half-life study with MG132 or leupeptin (*n* = 3). CHX, cycloheximide. (**B**) Immunoblotting showing levels of endogenous PIAS proteins and V5-HECTD2 after ectopic HECTD2 plasmid expression (*n* = 3). (**C**) Endogenous PIAS1 protein half-life determination with empty plasmid or *HECTD2* expression (top panel); endogenous PIAS1 protein half-life determination with control (CON) shRNA or *HECTD2* shRNA expression (bottom panel) (*n* = 3). (**D**) In vitro ubiquitination assay. Purified E1 and E2 components were incubated with V5-PIAS1, HECTD2, and the full complement of ubiquitination reaction components (second lane) showing polyubiquitinated PIAS1 proteins (*n* = 2). (**E** to **G**) NF-κB promoter activity assays. 293T cells were cotransfected with Cignal NF-κB dual luciferase reporter plasmids along with empty or *HECTD2* plasmid or control shRNA, *HECTD2* shRNA, or *PIAS1* shRNA 24 hours before HECTD2 plasmid expression. Twenty-four hours later, cells were treated with LPS (10 μg/ml), TNF (10 ng/ml), or IFN-γ (10 ng/ml) for an additional 6 hours (F and G) or 18 hours. Cells were then collected and assayed for luciferase activity to evaluate NF-κB promoter activity. Means ± SEM (*n* = 3). (**H**) MLE cells were treated with LPS in a time- or dose-dependent manner; cells were then collected and assayed for HECTD2, PIAS, and actin immunoblotting. Endogenous HECTD2 was also immunoprecipitated (IP) and followed by PIAS1 and PIAS4 immunoblotting (*n* = 2). Source data in fig. S10 and table S2.

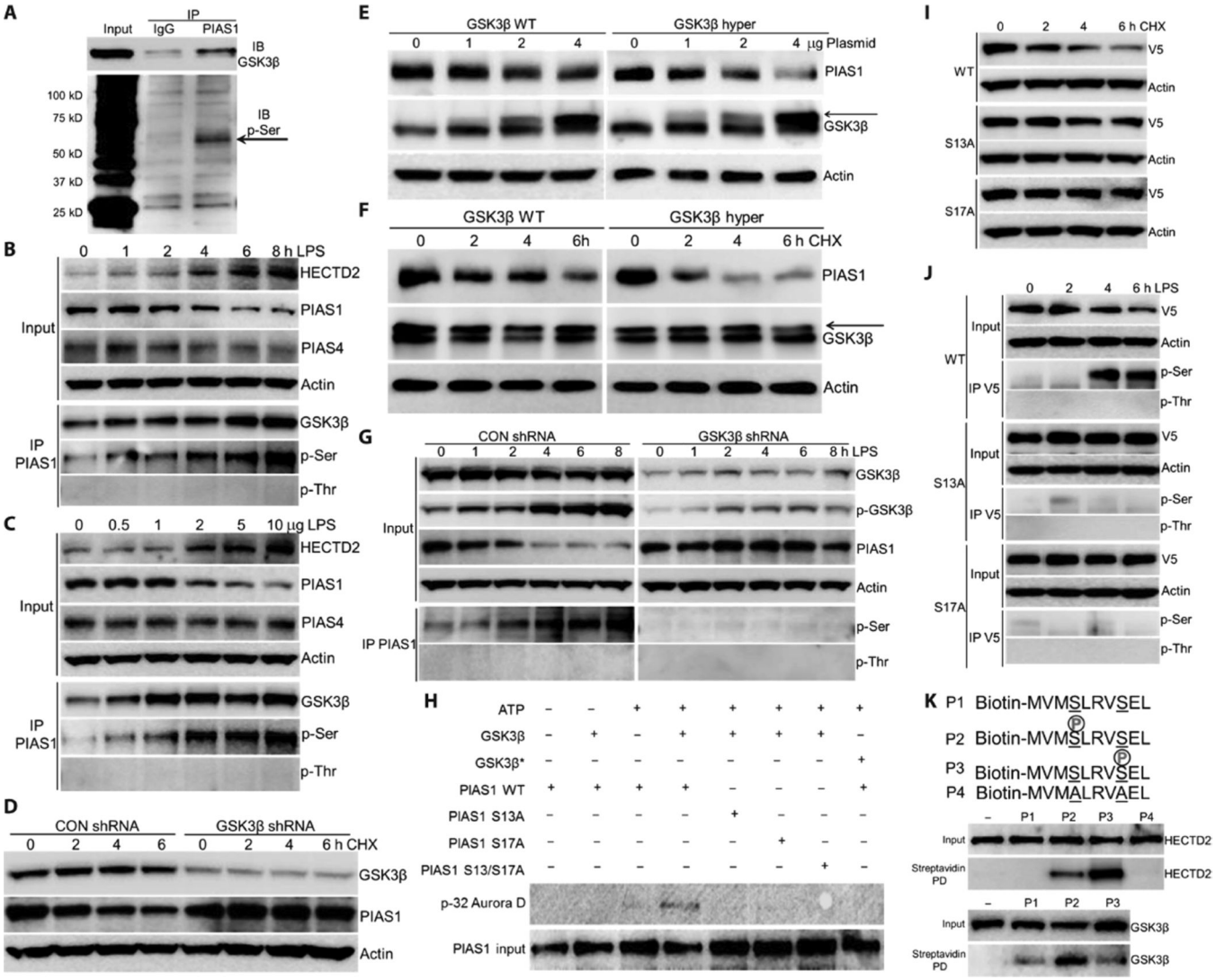

Fig. 2. PIAS1 phosphorylation is required for HECTD2 targeting

(**A**) Endogenous PIAS1 was immunoprecipitated and followed by GSK3β and phosphoserine antibody immunoblotting (IB) (*n* = 2). IgG, immunoglobulin G. (**B** and **C**) MLE cells were treated with LPS in a time- or dose-dependent manner; cells were then collected and assayed for HECTD2, PIAS, and actin immunoblotting. Endogenous PIAS1 was also immunoprecipitated and followed by GSK3β, phosphoserine, and phosphothreonine immunoblotting (*n* = 2). (**D**) Endogenous PIAS1 protein half-life determination with control shRNA or *GSK3*β shRNA overexpression (*n* = 3). (**E**) MLE cells were transfected with increasing amounts of WT or constitutively activated *GSK3*β hypermutant plasmids for 18 hours before PIAS1 immunoblotting. The arrow indicates the overexpressed GSK3β (*n* = 2). (**F**) Endogenous PIAS1 protein half-life determination with WT *GSK3*β or hyperactive *GSK3*β plasmid overexpression. Arrow indicates the overexpressed GSK3β (*n* = 2). (**G**) Immunoblotting showing levels of endogenous GSK3β and PIAS1 protein in MLE cells transfected with either control shRNA or *GSK3*β shRNA followed by LPS treatment. Endogenous PIAS1 was also immunoprecipitated and followed

by phosphoserine and phosphothreonine immunoblotting. (**H**) In vitro GSK3β kinase assay using PIAS1 as a substrate. GSK3β*, heat-inactivated GSK3β (n = 2). (**I**) Protein half-life of WT, S13A, and S17A PIAS1 (n = 3). (**J**) MLE cells were transfected with WT, S13A, or S17A PIAS1 before being treated with LPS for up to 6 hours. Cells were then collected and assayed for V5-PIAS1. Overexpressed V5-PIAS1 was also immunoprecipitated using V5 antibody and followed by phosphoserine immunoblotting (n = 2). (**K**) Four biotin-labeled peptides were prebound to streptavidin and served as the bait for HECTD2 or GSK3β binding. After washing, proteins were eluted and processed for V5-HECTD2 or GSK3β immunoblotting (n = 2). Source data in fig. S11.

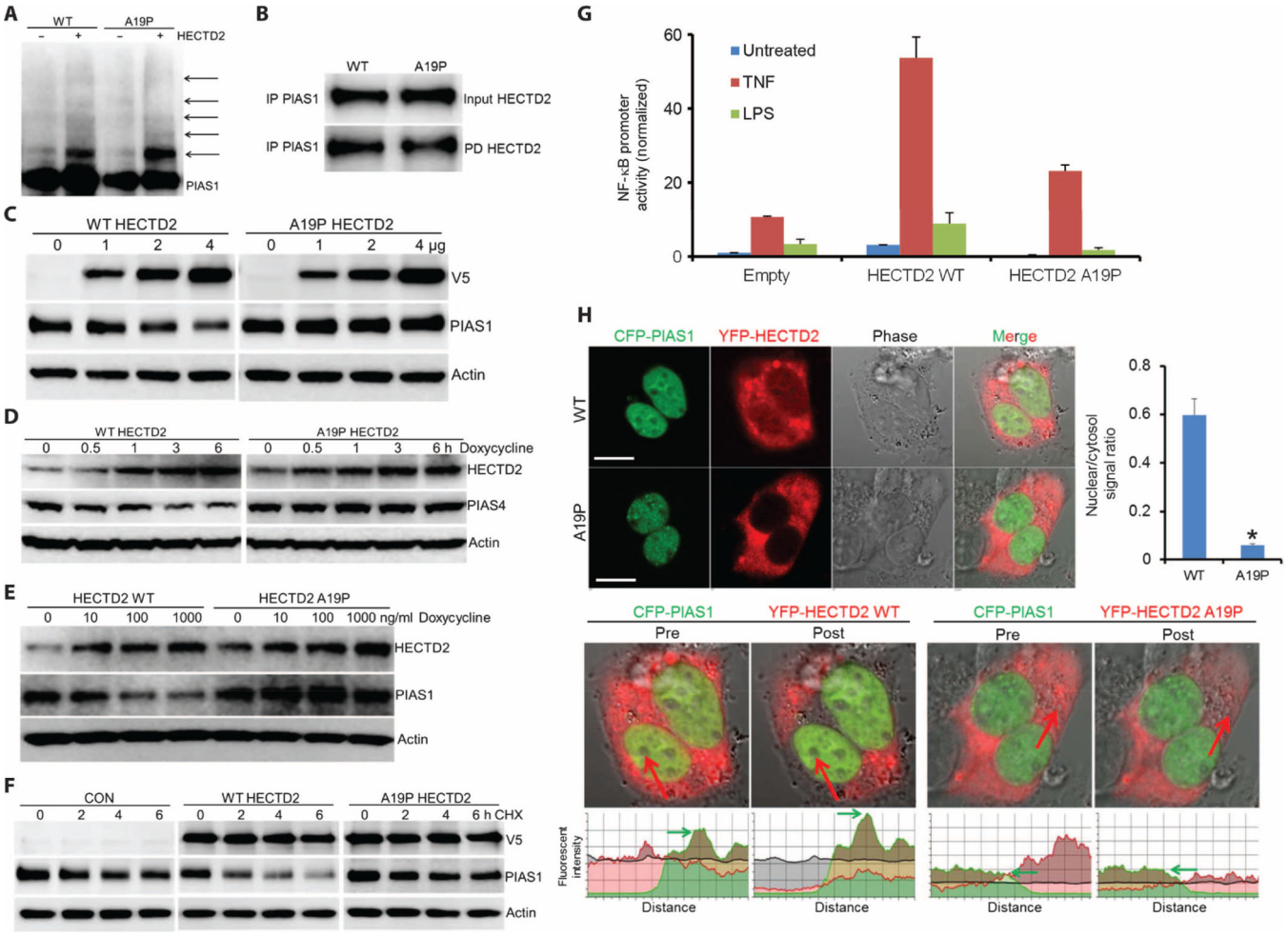

Fig. 3. HECTD2 contains a naturally occurring polymorphism at A19, which mislocalizes to the cytosol

(**A**) In vitro ubiquitination assay using V5-PIAS1 as the substrate and HECTD2^{WT} and HECTD2^{A19P} as the E3 ligase (*n* = 3). (**B**) Endogenous PIAS1 protein was immunoprecipitated from cell lysate using PIAS1 antibody and coupled to proteinA/G beads. PIAS1 beads were then incubated with in vitro synthesized products expressing his-V5-HECTD2 mutants (top). After washing, proteins were eluted and processed for V5-HECTD2 immunoblotting (bottom) (*n* = 2). (**C**) MLE cells were transfected with increasing amounts of *WT* or *A19P HECTD2* plasmids for 18 hours before being assayed for PIAS1 protein immunoblotting (*n* = 3). (**D** and **E**) MLE cells were transfected with an inducible *HECTD2^{WT}* or *HECTD2^{A19P}* plasmid under control of exogenous doxycycline. Cells were treated with doxycycline for various times and dose. Cells were then collected, and cell lysates were analyzed for HECTD2 and PIAS1 by immunoblotting (*n* = 2). (**F**) Half-life study of endogenous PIAS1 uponHECTD2^{WT} orHECTD2^{A19P} overexpression (*n*=2). (**G**) 293Tcells were cotransfected with Cignal NF-κB reporter plasmids and empty, *HECTD2^{WT}*, or *HECTD2^{A19P}* plasmid for 18 hours. Cells were then exposed to LPS or TNF for additional 18 hours before being assayed for NF-κB promoter activity. Means ± SEM (*n* = 3). (**H**) MLE cells were cotransfected with CFP-*PIAS1* and YFP-*HECTD2^{WT}* or YFP-

HECTD2^{A19P}. YFP-*HECTD2*^{WT} and YFP-*HECTD2*^{A19P} nuclear/cytosol fluorescent signals were measured and quantified ($n > 20$, right graph, $*P < 0.0001$ compared to WT). Cells were also subjected to irreversible photobleaching of YFP acceptor signal using a 514-nm laser. The emission fluorescence levels of both the donor CFP-PIAS1 and acceptor YFP-HECTD2^{WT} or YFP-HECTD2^{A19P} before and after acceptor photobleaching are shown in the lower panel; the region of interest across the nucleus is marked with a red arrow. The green arrow on the graph indicates donor CFP-PIAS1 signal before and after the photobleaching. Scale bar, 10 μm ($n > 10$). Source data in fig. S12 and table S3.

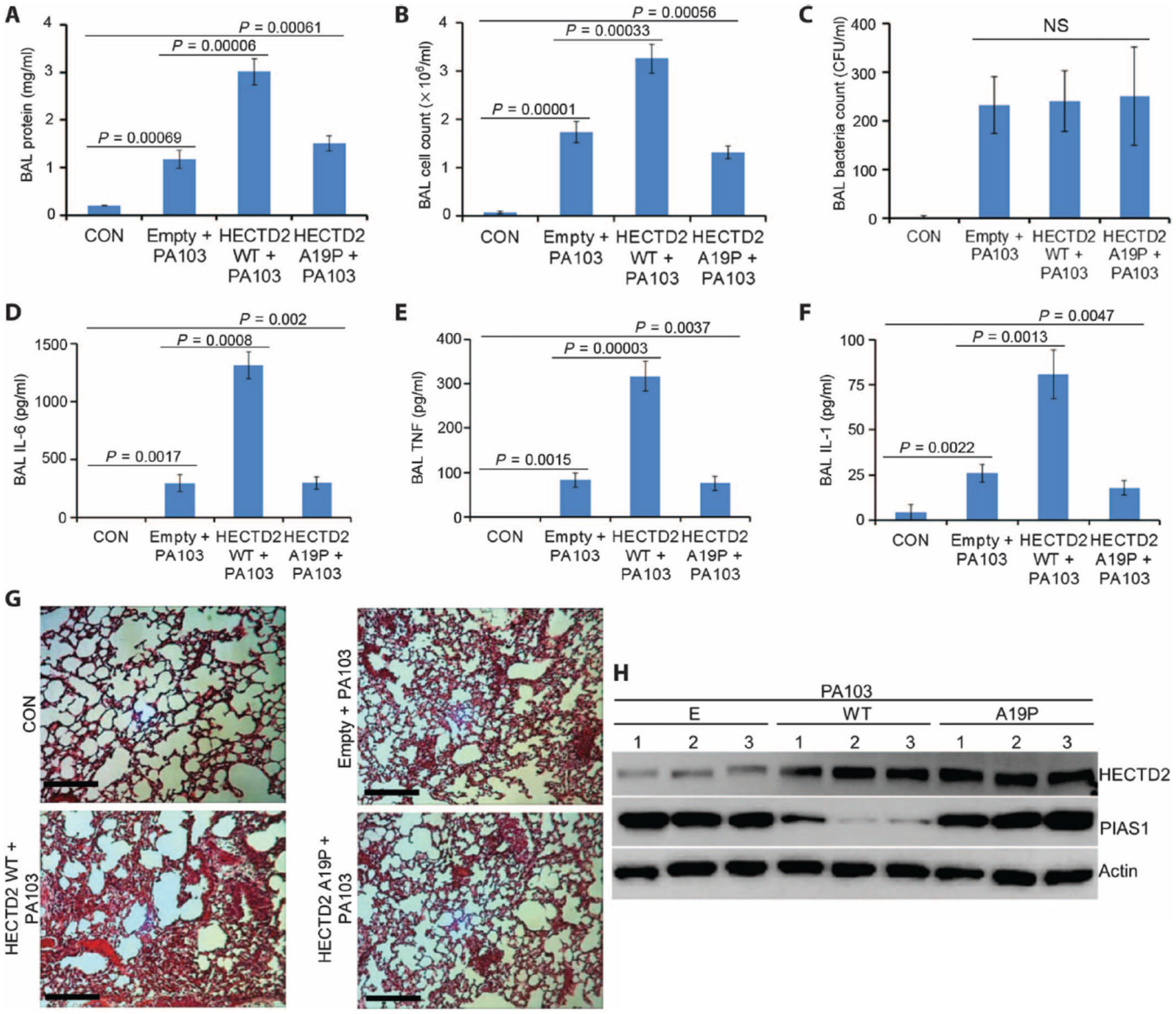

Fig. 4. HECTD2^{A19P} is a loss-of-function E3 ligase polymorphism in vivo

C57BL/6J mice were administered intratracheally with Lenticontrol, Lenti-*HECTD2*^{WT}, or Lenti-*HECTD2*^{A19P} [10^7 plaque-forming units (PFU) per mouse] for 144 hours, and mice were inoculated intratracheally with PA103 (10^4 PFU per mouse) for 18 hours. Mice were then euthanized, and lungs were lavaged with saline, harvested, and then homogenized. (**A** to **C**) Lavage protein, cell count, and bacteria count were measured. BAL, bronchoalveolar lavage. (**D** to **F**) Lavage cytokine secretion was measured. IL-6, interleukin-6. (**G**) Hematoxylin and eosin (H&E) staining was performed on lung samples from (A). Scale bar, 100 μm; original magnification, ×10. (**H**) PIAS1, HECTD2, and actin immunoblots from homogenized lung samples. Data are average of two experiments (Student's *t* test on means ± SEM). (A to G) *n* = 5 to 12 mice per group. Source data in fig. S13 and table S4.

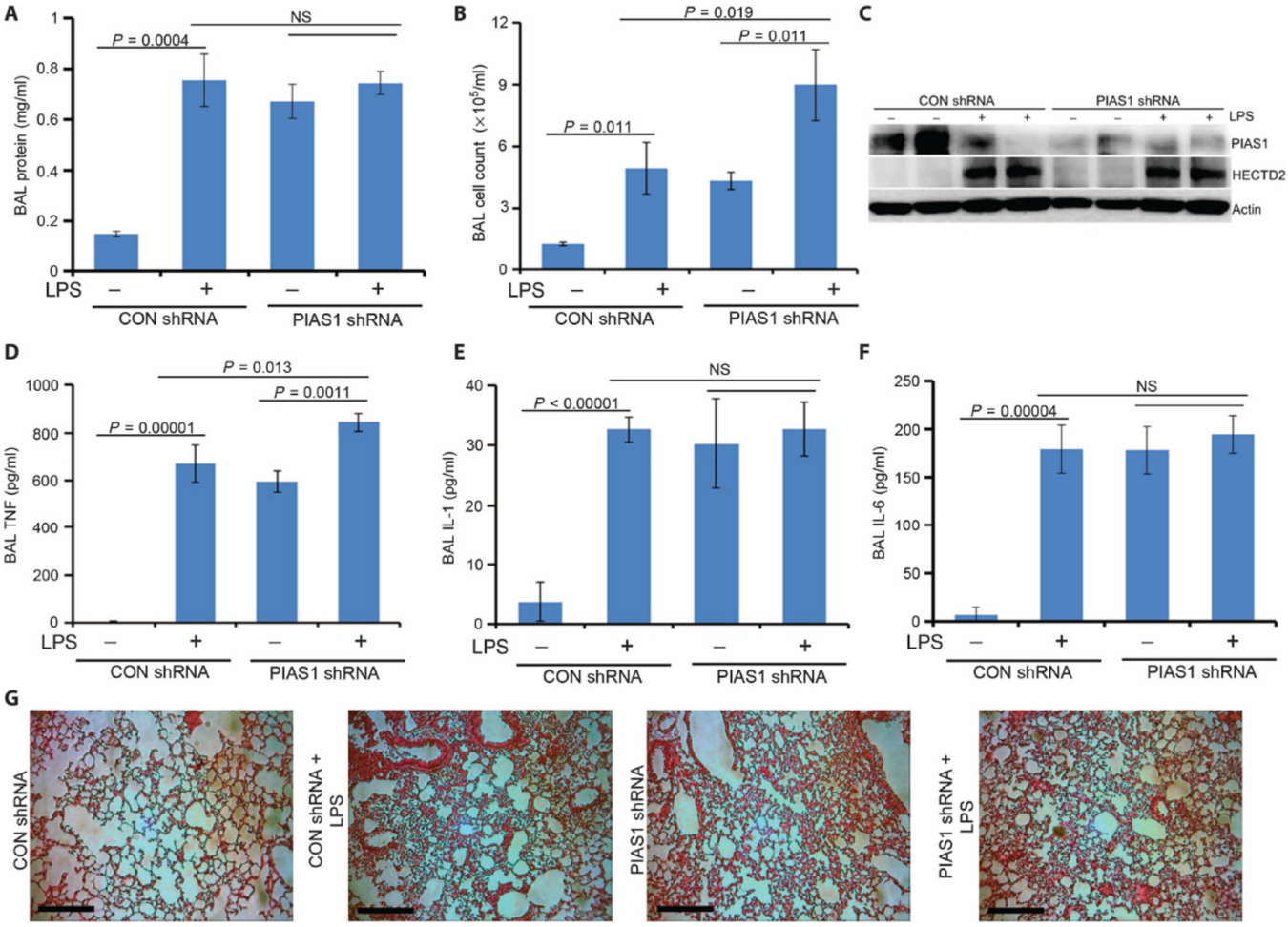

Fig. 5. PIAS1 knockdown induces lung injury in vivo

C57BL/6J mice were infected intratracheally with Lenti-control shRNA or Lenti-*PIAS1* shRNA (10^7 PFU per mouse) for 144 hours, and mice were inoculated with LPS (intratracheally, 3 mg/kg) for 18 hours. Mice were euthanized, and lungs were lavaged with saline, harvested, and then homogenized. (**A** to **C**) Lavage protein, cell count, and lung protein immunoblots were measured. (**D** to **F**) Lavage cytokine secretion was measured. (**G**) H&E staining was performed on lung samples from (A). Scale bar, 100 μm; original magnification, ×10 (Student's *t* test on means ± SEM). (A to G) $n = 5$ to 7 mice per group. Source data in fig. S13 and table S5.

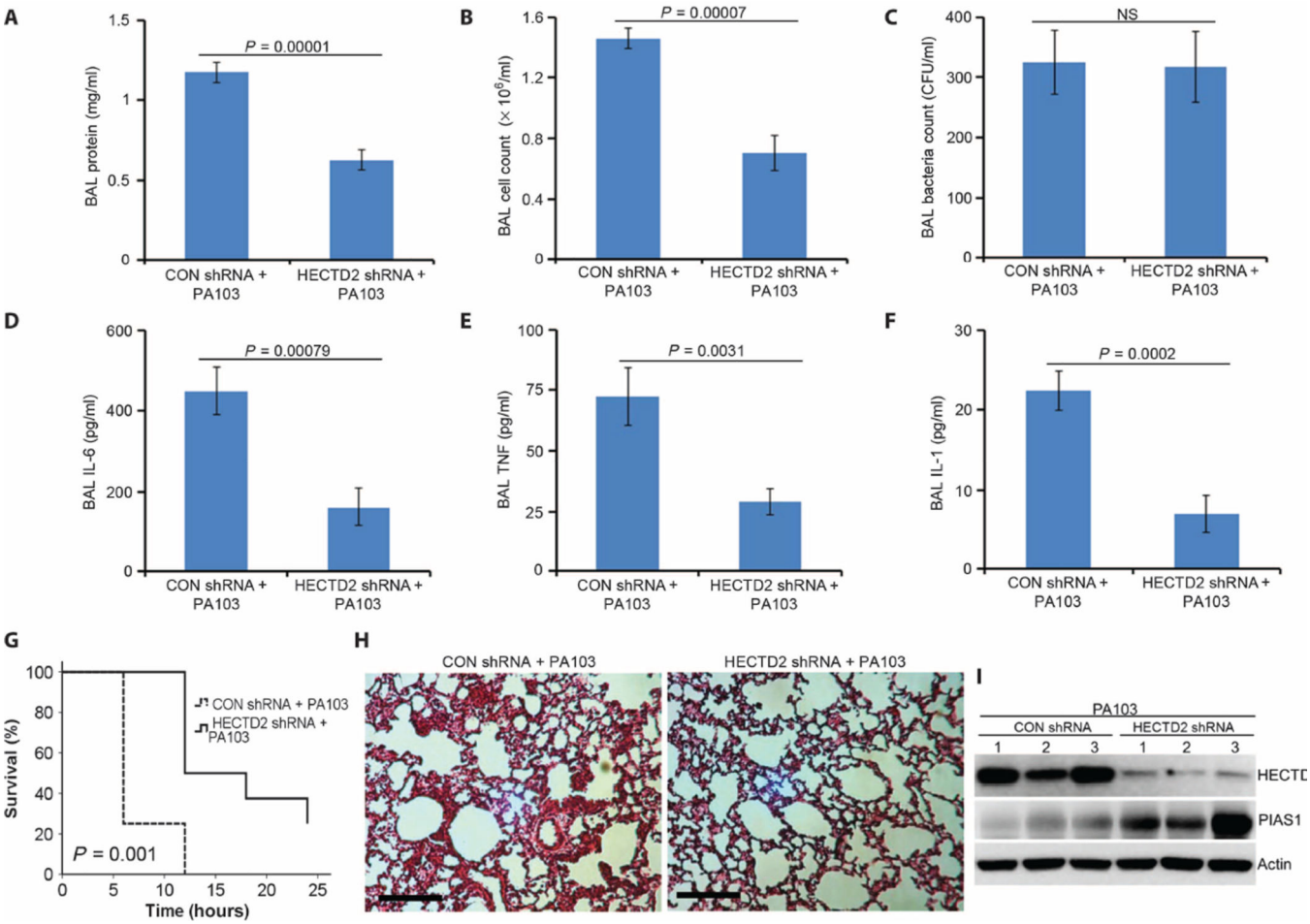

Fig. 6. HECTD2 knockdown ameliorates *Pseudomonas*-induced lung injury in vivo

C57BL/6J mice were infected intratracheally with Lenti-control shRNA or Lenti-*HECTD2* shRNA (10^7 PFU per mouse) for 144 hours, and mice were inoculated with PA103 [10^4 colony-forming units (CFU) per mouse] for 18 hours. Mice were euthanized, and lungs were lavaged with saline, harvested, and then homogenized. (**A** to **C**) Lavage protein, cell count, and bacteria count were measured. (**D** to **F**) Lavage cytokine secretion was measured. (**G**) Survival studies of mice that were administered PA103 (intratracheally, 10^5 PFU permouse, n = 8 mice per group) were determined (time, hours). Mice were carefully monitored over time; moribund, preterminal animals were immediately euthanized and recorded as deceased. Kaplan-Meier survival curves were generated using SPSS software (P=0.001). (**H**) H&E staining was performed on lung samples from (A). (**I**) PIAS1, HECTD2, and actin immunoblots from homogenized lung samples. Scale bar, 100 μm; original magnification, ×10. Data are average of two experiments (Student's t test on means ± SEM). (A to G) n = 6 to 9 mice per group. NS, not significant. Source data in fig. S13 and table S6.

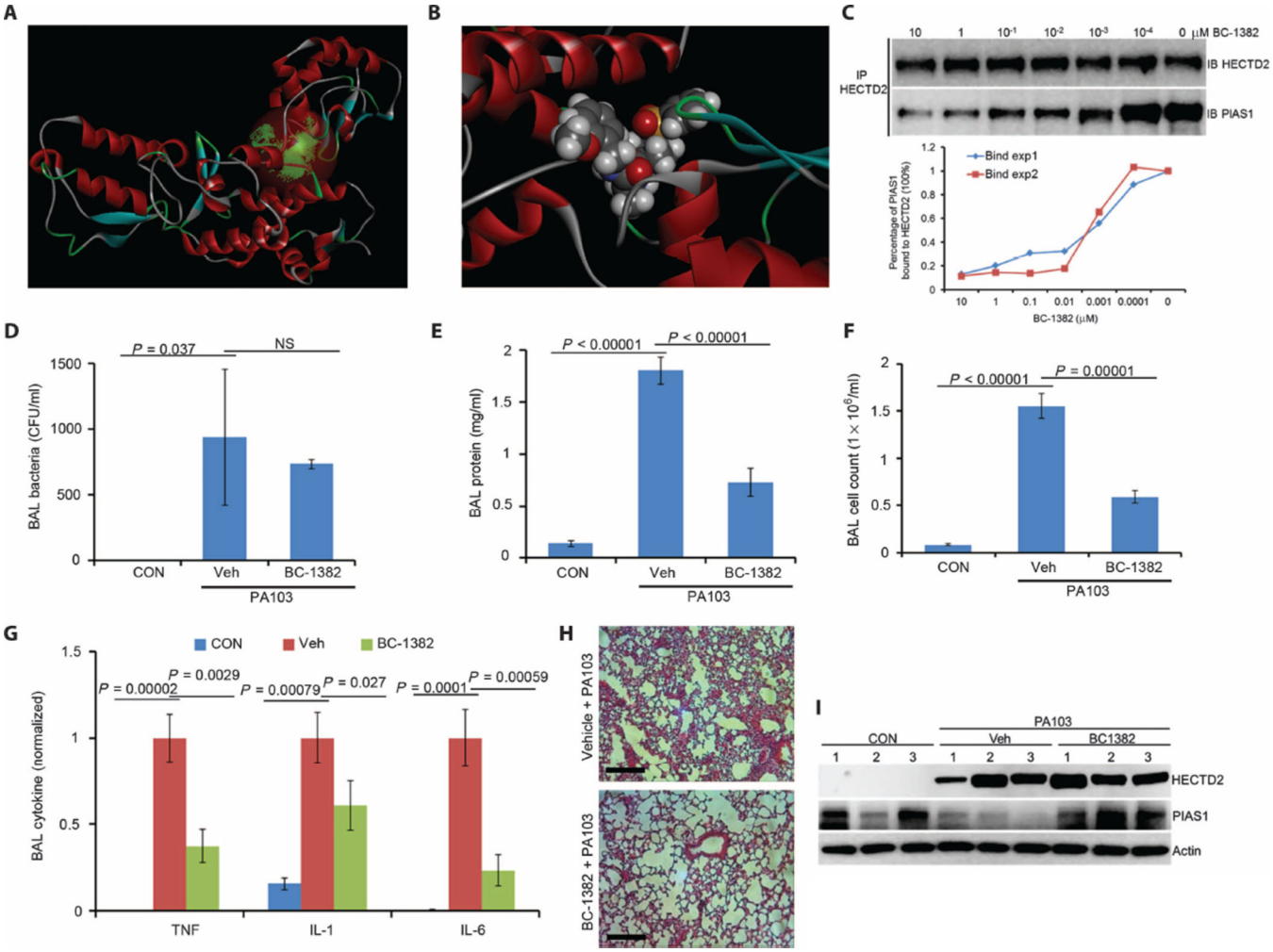

Fig. 7. Anti-inflammatory activity of a HECTD2 small-molecule inhibitor

(**A**) Structural analysis of the *HECTD2-HECT domain* revealed a major cavity within the C terminus of the *HECT domain*. (**B**) Docking study of candidate inhibitor BC-1382 with the *HECTD2-HECT domain*. (**C**) HECTD2 protein was immunoprecipitated using HECTD2 antibody and captured with protein A/G beads from MLE lysates. HECTD2 beads were extensively washed before exposure to BC-1382 at different concentrations (10^{-4} to 10 μM). Purified PIAS1 protein was then incubated with drug bound to HECTD2 beads overnight. Beads were washed, and proteins were eluted and resolved on SDS–polyacrylamide gel electrophoresis. The relative amounts of PIAS1 detected in the pull-downs were normalized to loading and quantified ($n = 2$). (**D** to **H**) C57BL/6J mice were infected intratracheally with PA103 (10^4 PFU per mouse). BC-1382 was given through intraperitoneal injection (10 mg/kg) at the same time. Eighteen hours later, mice were sacrificed, and lungs were lavaged with saline, harvested, and then homogenized. Lavage bacterial count, protein, cell count, and cytokine secretion were measured in (D) to (G). (H) H&E staining was performed on lung samples (scale bar, 100 μm; original magnification, ×10). (**I**) PIAS1, HECTD2, and actin immunoblots from homogenized lung samples. Data are average of two experiments

(Student's *t* test on means ± SEM). (D to H) *n* = 5 to 10 mice per group. Source data in fig. S13 and table S7.

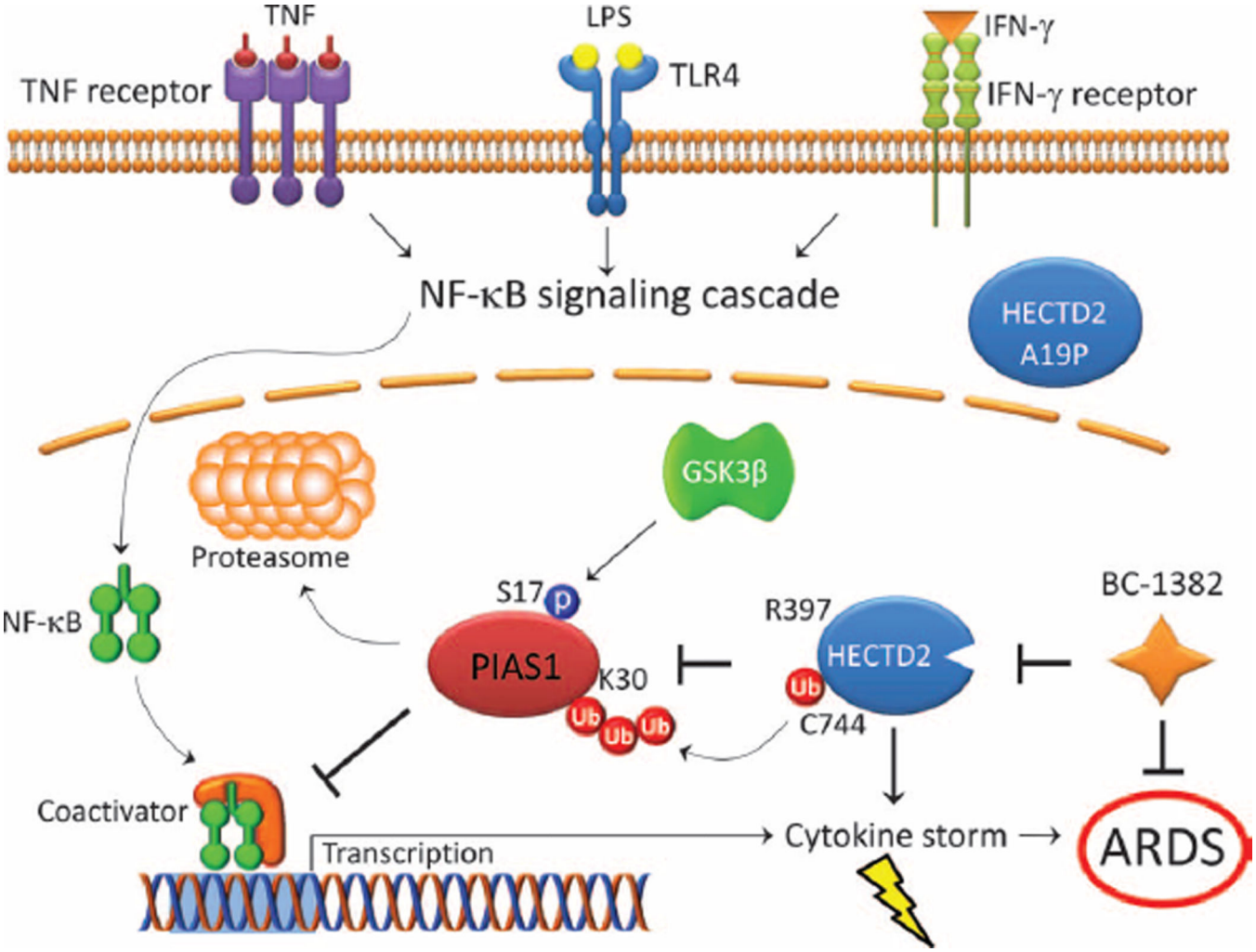

Fig. 8. One mechanism by which microbial infection or stimuli can robustly trigger inflammation is to decrease anti-inflammatory proteins such as PIAS1 in cells

Specifically, during microbial infection, HECTD2 (R397) targets PIAS1 for its ubiquitination at K30; this process is facilitated by GSK3β phosphorylation of PIAS1 at S17. In this pathway, WT HECTD2 potently activates cytokine-driven inflammation, whereas we identified a naturally occurring, mislocalized, hypofunctional variant of HECTD2 (*A19P*) that lowers the amount of cytokine secretion. A small-molecule HECTD2 inhibitor, BC-1382, decreased inflammation in an animal model of ARDS by antagonizing the actions of HECTD2 on PIAS1, allowing PIAS1 to continue to suppress cytokine signaling.

Table 1

rs7081569 SNP

Chromosome 10 position	**91410493 (+)**
Sequence	GTGGCGGCG**G**/**C**CCGCGCCTGA
AA change	MSEAVRVPSPATPLVVAA**A**/**P**APEERKGKESEREKLPPIVS

SNP analysis of HECTD2 protein indicating an A19P polymorphism (*rs7081569*) (noncoding strand is shown at http://www.ncbi.nlm.nih.gov/projects/SNP).

Table 2

Demographic characteristics by *rs7081569* polymorphism

	ARDS (*n* = 63)			*P*	1000 Genomes Project* (*n* = 1092)			*P*†
	CC (*n* = 0)	*CG* (*n* = 0)	*GG* (*n* = 63)		*CC* (*n* = 6)	*CG* (*n* = 174)	*GG* (*n* = 912)	
Male sex (%)	—	—	47	N/A	17	50	48	0.267
Race (%)								
European		95	33	28	36			
Hispanic		0	0	15	17			
Asian		0	17	24	27			
African		5	N/A	50	33	20	0.012	

*1000 Genomes Project, www.1000genomes.org/.

†*P* value by χ^2 test.

N/A, not applicable.

Table 3

Association of *rs7081569* polymorphism in ARDS cohort (Europeans, $n = 60$) and control Europeans ($n = 439$)

SNP genotype	ALI (%)	Healthy controls (%)	*P*
GG	60 (100)	328 (87)	
CG/CC	0 (0)	51 (13)	0.003

1000 Genomes Project, www.1000genomes.org/. *P* value by χ^2 test.